

ON SOME STRATEGIES FOR COMPUTER SIMULATION OF THE WAVE PROPAGATION USING FINITE DIFFERENCES

II. MULTI-DIMENSIONAL FDTD METHOD

Ľubomír Šumichrast *

Some strategies used in the computer simulation of wave phenomena by means of finite differences in time-domain (FDTD) method are reviewed and discussed here. It is shown that the wave equation in its discretised form possesses different properties in comparison with the true differential formulation. In this part the issues of stability and numerical dispersion for two- and three-dimensional case of wave propagation in homogeneous space are thoroughly investigated.

Key words: wave phenomena, computer simulation, finite differences in time domain (FDTD) method

1 INTRODUCTION

As discussed in part one of this tutorial review [1] the computer simulation of electromagnetic wave propagation is a subject of standing interest. The approximation of derivatives by finite differences in Maxwell equations is one of the most transparent and straightforward methods used. The fundamentals have been laid down in the seminal work of Yee [2] on the explicit finite-differences-in-time-domain (FDTD) method for vectorial wave components in three dimensions. The staggered three-dimensional discretisation grid introduced for three dimensional Maxwell equations in [2] and eventually its modifications [3] remained preserved in all other methods up to now. The main drawback — the conditional stability of the explicit FDTD method — has been overcome by introducing implicit Crank-Nicolson formulation of pertaining equations. Since the solution of the full set of equations for Crank-Nicolson algorithm is far beyond the possibilities of common computing machinery the approximate methods have been developed — the alternating-directions-implicit (ADI) approach [4–6] and the Crank-Nicolson-split-step (CNSS) approach [7, 8]. Character of both these approximations [9] will be shown. Both were in the last decade treated in numerous papers, the interested reader can easily find on himself, and their properties thoroughly investigated. In this tutorial paper the substantial features of the classical Yee FDTD method, together with one interesting modification of the discretisation grid in order to enlarge permissible time-step length [2] will be reviewed and analysed from the point of view of the power conservation and the numerical dispersion.

2 ELECTROMAGNETIC WAVE PROPAGATION IN HOMOGENEOUS SPACE

Multidimensional wave phenomena of electromagnetics are represented by the electromagnetic waves propagating in space. Electromagnetic fields in source-free homogeneous, isotropic and lossless media are described by the Maxwell equations

$$\begin{aligned} \varepsilon \frac{\partial \mathbf{E}(\mathbf{r}, t)}{\partial t} &= \text{rot } \mathbf{H}(\mathbf{r}, t), \\ \mu \frac{\partial \mathbf{H}(\mathbf{r}, t)}{\partial t} &= -\text{rot } \mathbf{E}(\mathbf{r}, t), \end{aligned} \quad (1)$$

for the electric and magnetic field intensities \mathbf{E} and \mathbf{H} , where \mathbf{r} is the radius vector and ε and μ are the permittivity and permeability of the medium. The vectorial quantities in the Cartesian coordinates have the components, $\mathbf{E} = \{E_x, E_y, E_z\}$, $\mathbf{H} = \{H_x, H_y, H_z\}$ and $\mathbf{r} = \{x, y, z\}$ is the radius vector.

The full three-dimensional set of vectorial equations (1) represented in six scalar equations consists of two triples of equations, first for $\{E_x, E_y, E_z\}$ and the second for $\{H_x, H_y, H_z\}$, the first and the last equation are

$$\begin{aligned} \varepsilon \frac{\partial E_x(x, y, z, t)}{\partial t} &= \\ = \frac{\partial H_z(x, y, z, t)}{\partial y} - \frac{\partial H_y(x, y, z, t)}{\partial z}, \end{aligned} \quad (2)$$

$$\begin{aligned} \mu \frac{\partial H_z(x, y, z, t)}{\partial t} &= \\ = \frac{\partial E_x(x, y, z, t)}{\partial y} - \frac{\partial E_y(x, y, z, t)}{\partial x}. \end{aligned} \quad (3)$$

The other four equations can be obtained by the cyclic permutation of all indices $\{x, y, z\}$ either in (2) or in (3).

* Slovak University of Technology, Institute of Electrical Engineering, Ilkovičova 3, SK-81219 Bratislava, Slovakia
lubomir.sumichrast@stuba.sk

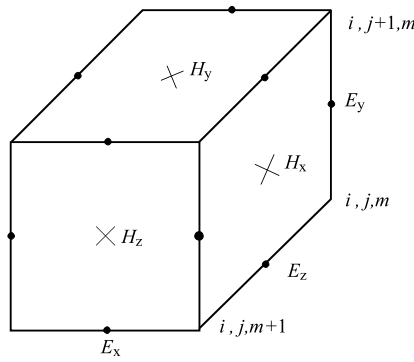


Fig. 1. Configuration of the staggered grid of Yee [2]

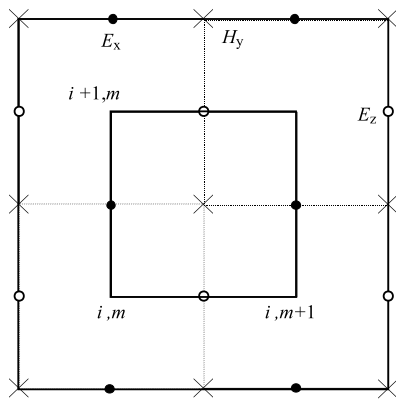


Fig. 2. Configuration of the two-dimensional Yee grid

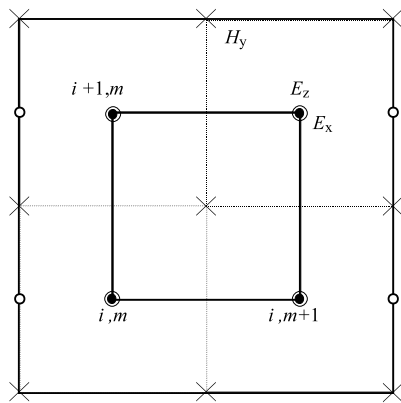


Fig. 3. Discretisation configuration accordingly [3]

In the two-dimensional case, when both \mathbf{E} and \mathbf{H} are independent from $eg\ y$, *ie* $\mathbf{E} = \mathbf{E}(x, z, t)$, $\mathbf{H} = \mathbf{H}(x, z, t)$, the six equations of the type (2) and (3) lead to two independent triples of equations, the first one for the transversal electric (TE) type of the field

$$\begin{aligned} \mu \frac{\partial H_y}{\partial t} &= \frac{\partial E_z}{\partial x} - \frac{\partial E_x}{\partial z}, \\ \varepsilon \frac{\partial E_z}{\partial t} &= \frac{\partial H_y}{\partial x}, \\ \varepsilon \frac{\partial E_x}{\partial t} &= -\frac{\partial H_y}{\partial z}, \end{aligned}$$

and the second one for the transversal magnetic (TM) type of the field

$$\begin{aligned} \varepsilon \frac{\partial E_y}{\partial t} &= \frac{\partial H_x}{\partial z} - \frac{\partial H_z}{\partial x}, \\ \mu \frac{\partial H_z}{\partial t} &= -\frac{\partial E_y}{\partial x}, \\ \mu \frac{\partial H_x}{\partial t} &= \frac{\partial E_y}{\partial z}, \end{aligned} \tag{5}$$

respectively.

From (1) one obtains two wave equations

$$\mu \varepsilon \frac{\partial^2 \mathbf{H}(\mathbf{r}, t)}{\partial t^2} = \nabla^2 \mathbf{H}(\mathbf{r}, t) - \text{grad div } \mathbf{H}(\mathbf{r}, t), \tag{6}$$

$$\mu \varepsilon \frac{\partial^2 \mathbf{E}(\mathbf{r}, t)}{\partial t^2} = \nabla^2 \mathbf{E}(\mathbf{r}, t) - \text{grad div } \mathbf{E}(\mathbf{r}, t). \tag{7}$$

For a simple case of $\text{div } \mathbf{H}(\mathbf{r}, t) = 0$ and $\text{div } \mathbf{E}(\mathbf{r}, t) = 0$ the wave equation for any Cartesian component of vectors \mathbf{E} and \mathbf{H} takes the form

$$\frac{1}{c^2} \frac{\partial^2 f(\mathbf{r}, t)}{\partial t^2} = \frac{\partial^2 f(\mathbf{r}, t)}{\partial x^2} + \frac{\partial^2 f(\mathbf{r}, t)}{\partial y^2} + \frac{\partial^2 f(\mathbf{r}, t)}{\partial z^2}. \tag{8}$$

The general solution of (8) takes the form of a plane wave $f(\mathbf{r}, t) = f(ct \mp \mathbf{n} \cdot \mathbf{r})$ propagating either in the positive or in the negative direction of the unit vector \mathbf{n} and $c = (\mu \varepsilon)^{-1/2}$.

3 DISCRETISATION OF THE MAXWELL EQUATIONS

The discrete values of $\{E_x, E_y, E_z, H_x, H_y, H_z\}$ are given, as depicted in Fig. 1, on the spatially staggered grid, designed by Yee [2]. The E -components are centered on the edges of the cube while the H -components are placed in the middle of the faces. In addition the E -components and the H -components are staggered along the time axis too, analogously to Fig. 1a in [1], *ie* the calculations are performed intermittently in discrete time instants $\mathbf{E} \Rightarrow (n + \frac{1}{2})\Delta_t$, $\mathbf{H} \Rightarrow n\Delta_t$. The calculation is thus performed for the values denoted as

$$E_x|_{i+\frac{1}{2}, j, m}^{n+\frac{1}{2}} = E_x((i + \frac{1}{2})\Delta_x, j\Delta_y, m\Delta_z, (n + \frac{1}{2})\Delta_t), \tag{9}$$

$$H_x|_{i, j+\frac{1}{2}, m+\frac{1}{2}}^n = H_x(i\Delta_x, (j + \frac{1}{2})\Delta_y, (m + \frac{1}{2})\Delta_z, n\Delta_t), \tag{10}$$

as well as for the values of other components: $E_y|_{i, j+\frac{1}{2}, m}^n$, $E_z|_{i, j, m+\frac{1}{2}}^{n+\frac{1}{2}}$, $H_y|_{i+\frac{1}{2}, j, m+\frac{1}{2}}^n$, $H_z|_{i+\frac{1}{2}, j+\frac{1}{2}, m}^n$ – positioned on edges and faces as given by the cyclic permutation of $\frac{1}{2}$ in the spatial indices.

(4)

For the sake of simplicity, in what follows the normalised quantities $h_{x,y,z} = H_{x,y,z}\sqrt{Z_0}$, and $e_{x,y,z} = E_{x,y,z}/\sqrt{Z_0}$ are introduced, where $Z_0 = \sqrt{\mu/\varepsilon}$ is the wave impedance of homogeneous media. The discretised equations (2) and (3) then read

$$e_x|_{i+\frac{1}{2},j,m}^{n+\frac{1}{2}} - e_x|_{i+\frac{1}{2},j,m}^{n-\frac{1}{2}} = b_y(h_z|_{i+\frac{1}{2},j+\frac{1}{2},m}^n - h_z|_{i+\frac{1}{2},j-\frac{1}{2},m}^n) - b_z(h_y|_{i+\frac{1}{2},j,m+\frac{1}{2}}^n - h_y|_{i+\frac{1}{2},j,m-\frac{1}{2}}^n), \quad (11)$$

$$h_z|_{i+\frac{1}{2},j+\frac{1}{2},m}^{n+1} - h_z|_{i+\frac{1}{2},j+\frac{1}{2},m}^n = b_y(e_x|_{i+\frac{1}{2},j+1,m}^{n+\frac{1}{2}} - e_x|_{i+\frac{1}{2},j,m}^{n+\frac{1}{2}}) - b_x(e_y|_{i+1,j+\frac{1}{2},m}^{n+\frac{1}{2}} - e_y|_{i,j+\frac{1}{2},m}^{n+\frac{1}{2}}), \quad (12)$$

where $b_{x,y,z} = c\Delta_t/\Delta_{x,y,z}$ are the Courant numbers along the respective axis. The equations analogous to (11) and (12) for the other four components are obtained by a cyclic permutation of component indices (x, y, z) and by a cyclic permutation of $\frac{1}{2}$ in the spatial indices (i, j, m) .

The in-time forward-marching algorithm provided by (11) and (12) proceeds in a ‘‘leapfrog’’ way, ie the values $e_{x,y,z}|^{n+\frac{1}{2}}$, $h_{x,y,z}|^{n+1}$, $e_{x,y,z}|^{n+\frac{3}{2}}$, $h_{x,y,z}|^{n+2}$, etc, in respective time layers are subsequently directly obtained from the values in two preceding time layers.

Since we want to show the principal properties of the respective algorithms, for the sake of simplicity in what follows the analysis will be mostly limited to the two-dimensional formulation only. For the TE-wave having the components $h_y|_{i+\frac{1}{2},m+\frac{1}{2}}^n$, $e_x|_{i+\frac{1}{2},m}^{n+\frac{1}{2}}$, $e_z|_{i,m+\frac{1}{2}}^{n+\frac{1}{2}}$ one obtains the formulae

$$h_y|_{i+\frac{1}{2},m+\frac{1}{2}}^{n+1} - h_y|_{i+\frac{1}{2},m+\frac{1}{2}}^n = b_x(e_z|_{i+1,m+\frac{1}{2}}^{n+\frac{1}{2}} - e_z|_{i,m+\frac{1}{2}}^{n+\frac{1}{2}}) - b_z(e_x|_{i+\frac{1}{2},m+1}^{n+\frac{1}{2}} - e_x|_{i+\frac{1}{2},m}^{n+\frac{1}{2}}), \quad (13)$$

$$e_z|_{i,m+\frac{1}{2}}^{n+\frac{1}{2}} - e_z|_{i,m+\frac{1}{2}}^{n-\frac{1}{2}} = b_x(h_y|_{i+\frac{1}{2},m+\frac{1}{2}}^n - h_y|_{i-\frac{1}{2},m+\frac{1}{2}}^n), \quad (14)$$

$$e_x|_{i+\frac{1}{2},m}^{n+\frac{1}{2}} - e_x|_{i+\frac{1}{2},m}^{n-\frac{1}{2}} = -b_z(h_y|_{i+\frac{1}{2},m+\frac{1}{2}}^n - h_y|_{i+\frac{1}{2},m-\frac{1}{2}}^n), \quad (15)$$

while for the TM-wave having the components $e_y|_{i,m}^{n+\frac{1}{2}}$, $h_x|_{i,m+\frac{1}{2}}^n$, $h_z|_{i+\frac{1}{2},m}^n$ one arrives to

$$e_y|_{i,m}^{n+\frac{1}{2}} - e_y|_{i,m}^{n-\frac{1}{2}} = b_z(h_x|_{i,m+\frac{1}{2}}^n - h_x|_{i,m-\frac{1}{2}}^n) - b_x(h_z|_{i+\frac{1}{2},m}^n - h_z|_{i-\frac{1}{2},m}^n), \quad (16)$$

$$h_z|_{i+\frac{1}{2},m}^{n+1} - h_z|_{i+\frac{1}{2},m}^n = b_x(e_y|_{i+1,m}^{n+\frac{1}{2}} - e_y|_{i,m}^{n+\frac{1}{2}}), \quad (17)$$

$$h_x|_{i,m+\frac{1}{2}}^{n+1} - h_x|_{i,m+\frac{1}{2}}^n = b_z(e_y|_{i,m+1}^{n+\frac{1}{2}} - e_y|_{i,m}^{n+\frac{1}{2}}). \quad (18)$$

Besides the Yee’s staggered grid there are also different possible discretisation configurations possible. One proposed in [3] is a modification of Yee’s grid depicted in Fig. 2 for the TE wave, where, as seen from Fig. 3, the

discretisation points for E_x and E_z are half-step shifted into corners of the basic cell, ie both E_x as well as E_z are defined in the same grid points. Then we again have the forward-marching explicit algorithm for the normalised grid values $h_y|_{i+\frac{1}{2},m+\frac{1}{2}}^n$, $e_x|_{i,m}^{n+\frac{1}{2}}$, $e_z|_{i,m}^{n+\frac{1}{2}}$ and centered difference equations expressed by

$$2(h_y|_{i+\frac{1}{2},m+\frac{1}{2}}^{n+1} - h_y|_{i+\frac{1}{2},m+\frac{1}{2}}^n) = b_x(e_z|_{i+1,m}^{n+\frac{1}{2}} - e_z|_{i,m}^{n+\frac{1}{2}} + e_z|_{i+1,m+1}^{n+\frac{1}{2}} - e_z|_{i,m+1}^{n+\frac{1}{2}}) - b_z(e_x|_{i,m+1}^{n+\frac{1}{2}} - e_x|_{i,m}^{n+\frac{1}{2}} + e_x|_{i+1,m+1}^{n+\frac{1}{2}} - e_x|_{i+1,m}^{n+\frac{1}{2}}), \quad (19)$$

$$2(e_z|_{i,m}^{n+\frac{1}{2}} - e_z|_{i,m}^{n-\frac{1}{2}}) = b_x(h_y|_{i+\frac{1}{2},m-\frac{1}{2}}^n - h_y|_{i-\frac{1}{2},m-\frac{1}{2}}^n + h_y|_{i+\frac{1}{2},m+\frac{1}{2}}^n - h_y|_{i-\frac{1}{2},m+\frac{1}{2}}^n) \quad (20)$$

$$2(e_x|_{i,m}^{n+\frac{1}{2}} - e_x|_{i,m}^{n-\frac{1}{2}}) = -b_z(h_y|_{i-\frac{1}{2},m+\frac{1}{2}}^n - h_y|_{i-\frac{1}{2},m-\frac{1}{2}}^n + h_y|_{i+\frac{1}{2},m+\frac{1}{2}}^n - h_y|_{i+\frac{1}{2},m-\frac{1}{2}}^n). \quad (21)$$

4 POWER CONSERVATION AND NUMERICAL DISPERSION OF THE EXPLICIT SCHEMES

The von Neumann stability analysis as elucidated in [1] leads in the two dimensional case for *eg* time-harmonic plane TE-wave to

$$e_x|_{i+\frac{1}{2},m}^{n+\frac{1}{2}} = e_{x0}\xi^{n+\frac{1}{2}} \exp\{jk_x(i+\frac{1}{2})\Delta_x\} \exp(jk_z m\Delta_z),$$

$$e_z|_{i,m+\frac{1}{2}}^{n+\frac{1}{2}} = e_{z0}\xi^{n+\frac{1}{2}} \exp(jk_x i\Delta_x) \exp\{jk_z(m+\frac{1}{2})\Delta_z\},$$

$h_y|_{i+\frac{1}{2},m+\frac{1}{2}}^n = h_{y0}\xi^n \exp\{jk_x(i+\frac{1}{2})\Delta_x\} \exp\{jk_z(m+\frac{1}{2})\Delta_z\}$ with $\xi = \exp(-j\omega\Delta_t)$ and the wave number $k = \sqrt{k_x^2 + k_z^2}$.

After inserting into (13), (14) and (15) one obtains the equation

$$\xi^2 - 2[1 - 2(A_x^2 + A_z^2)]\xi + 1 = 0, \quad (22)$$

where

$$A_x = b_x \sin(\frac{1}{2}k_x\Delta_x), \quad (23)$$

$$A_z = b_z \sin(\frac{1}{2}k_z\Delta_z), \quad (24)$$

with the solution

$$\xi = [1 - 2(A_x^2 + A_z^2)] - j\sqrt{1 - [1 - 2(A_x^2 + A_z^2)]^2}. \quad (25)$$

In order to achieve the power conservation of the algorithm the expression under the square root sign must be positive leading thus to the condition

$$A_x^2 + A_z^2 \leq 1. \quad (26)$$

Due to the sampling theorem $k\Delta|_{x,z} = \pi$ holds for the maximum representable values of the wavenumbers k_x , k_z with the sampling intervals Δ_x , Δ_z , and therefore $A_{x,z}|_{\max} = c\Delta_t/\Delta_{x,z}$, leading to the ultimate power conservation condition (CFL condition (59) in [1] in two dimensions)

$$c\Delta_t\sqrt{\Delta_x^{-2} + \Delta_z^{-2}} \leq 1, \text{ or } \sqrt{b_x^2 + b_z^2} \leq 1. \quad (27)$$

It is noteworthy to mention that for the aspect ratio tan $\alpha = \Delta_z/\Delta_x$ and the diagonal of the discretisation cell $d = \sqrt{\Delta_x^2 + \Delta_z^2}$, (27) can be written as $c\Delta_t < \frac{1}{2}d \sin 2\alpha$, giving the maximum value $c\Delta_t|_{\max} = d/2 = \Delta/\sqrt{2}$ for the aspect ratio one, i.e. $\Delta = \Delta_x = \Delta_z$. On the other hand for $\Delta_x \ll \Delta_z$, or $\Delta_z \ll \Delta_x$, the maximum value is either $c\Delta_t|_{\max} \approx \Delta_x/2$, or $c\Delta_t|_{\max} \approx \Delta_z/2$. The maximum permitted time-step $\Delta_t|_{\max}$ thus generally depends also on the geometrical configuration of the discretisation cell.

If the CFL condition is met (25) yields for $\omega\Delta_t$ with $\omega\Delta_t = -\text{phase}(\xi)$

$$\omega\Delta_t = \arccos[1 - 2(A_x^2 + A_z^2)], \quad (28)$$

or written in a more familiar form

$$\frac{\sin^2(\frac{1}{2}\omega\Delta_t)}{c^2\Delta_t^2} = \frac{\sin^2(\frac{1}{2}k_x\Delta_x)}{\Delta_x^2} + \frac{\sin^2(\frac{1}{2}k_z\Delta_z)}{\Delta_z^2}. \quad (29)$$

The phase velocity $v_p(k) = \omega(k)/k$ and the group velocity $v_g(k) = d\omega(k)/dk$ of the simulated wave propagation

$$v_p(k) = \frac{1}{k\Delta_t} \arccos[1 - 2(A_x^2 + A_z^2)], \quad (30)$$

$v_g(k) =$

$$c \frac{A_x \cos(\frac{1}{2}k_x\Delta_x) \cos \eta + A_z \cos(\frac{1}{2}k_z\Delta_z) \sin \eta}{\sqrt{A_x^2 + A_z^2} \sqrt{1 - (A_x^2 + A_z^2)}}, \quad (31)$$

are not constant, they differ from the physical phase and group velocity $v_p = v_g = c$, and depend not only on the wavenumber k , $k = \sqrt{k_x^2 + k_z^2}$, $k_x = k \cos \eta$, $k_z = k \sin \eta$, but also on the direction of the wave propagation given by the angle η , leading thus to the artificial numerical dispersion given by (30) and (31).

Notice that the wavenumbers k_x , k_z can have only discrete values too, given by $k_x|_i = (2\pi i)/(M_x\Delta_x)$, $k_z|_m = (2\pi m)/(M_z\Delta_z)$, where $M_x \times M_z$ is the number of discretisation points in the computational window $(0, x_{\max}) \times (0, z_{\max})$, $x_{\max} = M_x\Delta_x$, $z_{\max} = M_z\Delta_z$. The discrete set of permissible wave vectors is given by $\mathbf{k}|_{i,m} = (\pm k_x|_i, \pm k_z|_m)$, $i = 1, 2, \dots, M_x/2$, $m = 1, 2, \dots, M_z/2$ since the highest representable wavenumber in respective direction is given by $k_{x,z}|_{\max} = \pi/\Delta_{x,z}$. There are thus exactly $M_x \times M_z$ permissible discrete propagation directions and any wave distribution in space can consist only of this discrete spectrum of plane waves.

This set of $\mathbf{k}|_{i,m}$ vectors in fact represents a reciprocal lattice pertaining to the discretisation grid.

For the discretisation scheme as proposed by Bi *et al* in [3] the von Neumann analysis leads instead of (25) to

$$\xi^2 - 2\{1 - 2[A_x^2 \cos^2(\frac{1}{2}k_z\Delta_z) + A_z^2 \cos^2(\frac{1}{2}k_x\Delta_x)]\}\xi + 1 = 0, \quad (32)$$

giving the condition of power conservation in the form

$$A_x^2 \cos^2(\frac{1}{2}k_z\Delta_z) + A_z^2 \cos^2(\frac{1}{2}k_x\Delta_x) \leq 1. \quad (33)$$

The maximum value in (33) is reached for $k_{x,y}\Delta_{x,y} = \pi/2$ leading to the less stringent condition on Δ_t

$$c\Delta_t\sqrt{\Delta_x^{-2} + \Delta_z^{-2}} \leq 2 \quad (34)$$

and of course to the different numerical dispersion properties given by

$$\omega\Delta_t = \arccos\{1 - 2[A_x^2 \cos^2(\frac{1}{2}k_z\Delta_z) + A_z^2 \cos^2(\frac{1}{2}k_x\Delta_x)]\}. \quad (35)$$

Notice the difference in phase velocities, the simulation using the grid in Fig. 3. leads for the same $k_{x,z}\Delta_{x,z}$ and $b_{x,z} = c\Delta_t/\Delta_{x,z}$ to lower phase velocity in simulated wave propagation than the grid in Fig. 2.

5 THE FULL IMPLICIT FORMULATION: CN-FDTD METHOD

In the matrix notation (1) reads

$$\begin{aligned} \varepsilon \frac{\partial}{\partial t} \mathbf{E} &= \mathbf{G} \cdot \mathbf{H}, \\ \mu \frac{\partial}{\partial t} \mathbf{H} &= -\mathbf{G} \cdot \mathbf{E}, \end{aligned} \quad (36)$$

where $\mathbf{E} = [E_x, E_y, E_z]^\top$ and $\mathbf{H} = [H_x, H_y, H_z]^\top$ are column vectors of the field components and \mathbf{G} is given as

$$\mathbf{G} = \mathbf{G}_1 - \mathbf{G}_2 = \begin{bmatrix} 0 & -\partial/\partial z & \partial/\partial y \\ \partial/\partial z & 0 & -\partial/\partial x \\ -\partial/\partial y & \partial/\partial x & 0 \end{bmatrix}, \quad (37)$$

where

$$\begin{aligned} \mathbf{G}_1 &= \begin{bmatrix} 0 & 0 & \partial/\partial y \\ \partial/\partial z & 0 & 0 \\ 0 & \partial/\partial x & 0 \end{bmatrix}, \\ \mathbf{G}_2 &= \begin{bmatrix} 0 & \partial/\partial z & 0 \\ 0 & 0 & \partial/\partial x \\ \partial/\partial y & 0 & 0 \end{bmatrix}. \end{aligned} \quad (38)$$

Combining normalised vectors \mathbf{E} and \mathbf{H} into one vector $\mathbf{f} = [e_x, e_y, e_z, h_x, h_y, h_z]^\top$, one arrives to the equation

$$c^{-1} \frac{\partial}{\partial t} \mathbf{f} = \mathbf{D} \cdot \mathbf{f}, \quad (39)$$

where \mathbf{D} is an 6×6 matrix

$$\mathbf{D} = \begin{bmatrix} 0 & \mathbf{G}_1 - \mathbf{G}_2 \\ \mathbf{G}_2 - \mathbf{G}_1 & 0 \end{bmatrix}, \quad (40)$$

that can be written also in the form

$$\mathbf{D} = \mathbf{D}_1 + \mathbf{D}_2 = \mathbf{D}_{12} - \mathbf{D}_{21} \quad (41)$$

where

$$\mathbf{D}_1 = \begin{bmatrix} \mathbf{0} & \mathbf{G}_1 \\ -\mathbf{G}_1 & \mathbf{0} \end{bmatrix}, \quad \mathbf{D}_2 = \begin{bmatrix} \mathbf{0} & -\mathbf{G}_2 \\ \mathbf{G}_2 & \mathbf{0} \end{bmatrix}, \quad (42)$$

$$\mathbf{D}_{12} = \begin{bmatrix} \mathbf{0} & \mathbf{G}_1 \\ \mathbf{G}_2 & \mathbf{0} \end{bmatrix}, \quad \mathbf{D}_{21} = \begin{bmatrix} \mathbf{0} & \mathbf{G}_2 \\ \mathbf{G}_1 & \mathbf{0} \end{bmatrix}. \quad (43)$$

Discrete Crank-Nicolson formulation of (39) with respect to the time derivative yields

$$\frac{\mathbf{f}^{n+1} - \mathbf{f}^n}{c\Delta_t} = \mathbf{D} \cdot \frac{\mathbf{f}^{n+1} + \mathbf{f}^n}{2}. \quad (44)$$

After the discretisation of the spatial variables in (44) using the Crank-Nicolson algorithm, one arrives to the set of six difference equations, of which the first and the last one in concise notation [8] read

$$2(e_x|^{n+1} - e_x|^n) = c\Delta_t(\delta_y h_z|^{n+1} + \delta_y h_z|^n - \delta_z h_y|^{n+1} - \delta_z h_y|^n) \quad (45)$$

$$2(h_z|^{n+1} - h_z|^n) = c\Delta_t(\delta_y e_x|^{n+1} + \delta_y e_x|^n - \delta_x e_y|^{n+1} - \delta_x e_y|^n) \quad (46)$$

and the other four are obtained by cyclic permutation of indices in (45) and (46).

The first-order difference operator δ in above formulas is defined for the integer indices using the forward differences and for the half-integer indices using the backward differences, *ie*

$$\delta a_n = \frac{a|_{n+1} - a|_n}{\Delta}, \quad \delta a_{n+\frac{1}{2}} = \frac{a|_{n+\frac{1}{2}} - a|_{n-\frac{1}{2}}}{\Delta}. \quad (47)$$

The second order operator is defined using the central differences

$$\delta^2 a_i = \frac{a|_{i+1} - 2a|_i + a|_{i-1}}{\Delta^2}, \quad (48)$$

$$\delta^2 a_{i+\frac{1}{2}} = \frac{a|_{i+\frac{3}{2}} - 2a|_{i+\frac{1}{2}} + a|_{i-\frac{1}{2}}}{\Delta}. \quad (49)$$

Thus the equations (45) and (46) in fact mean

$$2(e_x|_{i+\frac{1}{2},j,m}^{n+1} - e_x|_{i+\frac{1}{2},j,m}^n) = b_y \left(h_z|_{i+\frac{1}{2},j+\frac{1}{2},m}^{n+1} - h_z|_{i+\frac{1}{2},j-\frac{1}{2},m}^{n+1} + h_z|_{i+\frac{1}{2},j+\frac{1}{2},m}^n - h_z|_{i+\frac{1}{2},j-\frac{1}{2},m}^n \right) - b_z \left(h_y|_{i+\frac{1}{2},j,m+\frac{1}{2}}^{n+1} - h_y|_{i+\frac{1}{2},j,m-\frac{1}{2}}^{n+1} + h_y|_{i+\frac{1}{2},j,m+\frac{1}{2}}^n - h_y|_{i+\frac{1}{2},j,m-\frac{1}{2}}^n \right). \quad (50)$$

$$2(h_z|_{i+\frac{1}{2},j+\frac{1}{2},m}^{n+1} - h_z|_{i+\frac{1}{2},j+\frac{1}{2},m}^n) = b_y \left(e_x|_{i+\frac{1}{2},j+1,m}^{n+1} - e_x|_{i+\frac{1}{2},j,m}^{n+1} + e_x|_{i+\frac{1}{2},j,m}^n - e_x|_{i+\frac{1}{2},j+1,m}^n \right) - b_x \left(e_y|_{i+1,j+\frac{1}{2},m}^{n+1} - e_y|_{i,j+\frac{1}{2},m}^{n+1} + e_y|_{i,j+\frac{1}{2},m}^n - e_y|_{i+1,j+\frac{1}{2},m}^n \right). \quad (51)$$

Note that in (50) and (51) in contrast to (11) there is no staggering of the discrete values along the time axis.

If there are M spatial discretisation points along each axis x , y , and z , the solution of six unknowns from (50) (and subsequent five equations) requires for each simulation step inversion of the $(6M^3 \times 6M^3)$ sparse matrix. This is usually already for a moderate number of sampling points M (*eg* $M \approx 50$) not realizable task on the common computing machinery.

6 THE APPROXIMATE IMPLICIT FORMULATION: ADI- FDTD METHOD

Equation (44) can be put in the following form

$$\left\{ \mathbf{I} - \frac{c\Delta_t}{2}(\mathbf{D}_1 + \mathbf{D}_2) \right\} \mathbf{f}^{n+1} = \left\{ \mathbf{I} + \frac{c\Delta_t}{2}(\mathbf{D}_1 + \mathbf{D}_2) \right\} \mathbf{f}^n, \quad (52)$$

which can after some calculation be re-cast into the following form (see *eg* [7])

$$\left\{ \mathbf{I} - \frac{c\Delta_t}{2} \mathbf{D}_1 \right\} \left\{ \mathbf{I} - \frac{c\Delta_t}{2} \mathbf{D}_2 \right\} \mathbf{f}^{n+1} - \frac{c^2 \Delta_t^2}{4} \mathbf{D}_1 \cdot \mathbf{D}_2 \mathbf{f}^{n+1} = \left\{ \mathbf{I} + \frac{c\Delta_t}{2} \mathbf{D}_2 \right\} \left\{ \mathbf{I} + \frac{c\Delta_t}{2} \mathbf{D}_1 \right\} \mathbf{f}^n - \frac{c^2 \Delta_t^2}{4} \mathbf{D}_2 \cdot \mathbf{D}_1 \mathbf{f}^n. \quad (53)$$

Solving the full system of implicit equations (44), (52), (53) is far beyond the capabilities of common computational machinery. Therefore after having neglected last terms (of second order smallness) on the RHS and LHS of (53), one can split the resulting approximate equation

$$\left\{ \mathbf{I} - \frac{c\Delta_t}{2} \mathbf{D}_1 \right\} \left\{ \mathbf{I} - \frac{c\Delta_t}{2} \mathbf{D}_2 \right\} \mathbf{f}^{n+1} = \left\{ \mathbf{I} + \frac{c\Delta_t}{2} \mathbf{D}_2 \right\} \left\{ \mathbf{I} + \frac{c\Delta_t}{2} \mathbf{D}_1 \right\} \mathbf{f}^n \quad (54)$$

into two subsequent steps

$$\left\{ \mathbf{I} - \frac{c\Delta_t}{2} \mathbf{D}_2 \right\} \mathbf{f}^* = \left\{ \mathbf{I} + \frac{c\Delta_t}{2} \mathbf{D}_1 \right\} \mathbf{f}^n, \quad (55)$$

$$\left\{ \mathbf{I} - \frac{c\Delta_t}{2} \mathbf{D}_1 \right\} \mathbf{f}^{n+1} = \left\{ \mathbf{I} + \frac{c\Delta_t}{2} \mathbf{D}_2 \right\} \mathbf{f}^*, \quad (56)$$

where \mathbf{f}^* denotes the intermediate values after the first substep. As can be shown, \mathbf{f}^* approximates the value $\mathbf{f}^{n+1/2}$ and therefore it is often denoted in this way. This procedure is called Alternating-Directions-Implicit (ADI) FDTD method.

If there are M spatial discretisation points along each axis x , y , and z , then the algorithm for (55) and (56) can be organized in such a way that the full step Δ_t requires the inversion of the three tri-diagonal $M \times M$ matrices twice, *ie* for each half-step. As already mentioned the exact solution (52) requires inversion of the $(6M^3 \times 6M^3)$ sparse matrix. The difference in computational intensity between the problems characterised by $(6M^3 \times 6M^3)$ matrix and by three tri-diagonal $(M \times M)$ matrices is immense.

The first and the last equation of the set of six equations (55) for the first half-step after the spatial discretisation read

$$2(e_x|^{n+\frac{1}{2}} - e_x|^n) = c\Delta_t(\delta_y h_z|^{n+\frac{1}{2}} - \delta_z h_y|^n), \quad (57)$$

$$2(h_z|^{n+\frac{1}{2}} - h_z|^n) = c\Delta_t(\delta_y e_x|^{n+\frac{1}{2}} - \delta_x e_y|^n). \quad (58)$$

The first and the last equation of the set of six equations (56) for the second half-step read

$$2(e_x|^{n+1} - e_x|^{n+\frac{1}{2}}) = c\Delta_t(\delta_y h_z|^{n+\frac{1}{2}} - \delta_z h_y|^{n+1}), \quad (59)$$

$$2(h_z|^{n+1} - h_z|^{n+\frac{1}{2}}) = c\Delta_t(\delta_y e_x|^{n+\frac{1}{2}} - \delta_x e_y|^{n+1}). \quad (60)$$

The organisation of the algorithm into a tridiagonal matrix proceeds for the first half-step through the substitution of $h_z|^{n+\frac{1}{2}}$ from (58) into (57)

$$\begin{aligned} [4 - c^2 \Delta_t^2 \delta_y^2] e_x|^{n+\frac{1}{2}} = \\ 4e_x|^n + 2c\Delta_t[\delta_y h_z|^n - \delta_z h_y|^n] - c^2 \Delta_t^2 \delta_y \delta_x e_y|^n \end{aligned} \quad (61)$$

and the substitution of $e_x|^{n+\frac{1}{2}}$ from (57) into (58)

$$\begin{aligned} [4 - c^2 \Delta_t^2 \delta_x^2] h_z|^{n+\frac{1}{2}} = \\ 4h_z|^n + 2c\Delta_t[\delta_y e_x|^n - \delta_x e_y|^n] - c^2 \Delta_t^2 \delta_z \delta_y h_y|^n. \end{aligned} \quad (62)$$

For the second half step the similar procedure yields

$$\begin{aligned} [4 - c^2 \Delta_t^2 \delta_z^2] e_x|^{n+1} = 4e_x|^{n+\frac{1}{2}} + \\ 2c\Delta_t[\delta_y h_z|^{n+\frac{1}{2}} - \delta_z h_y|^{n+\frac{1}{2}}] - c^2 \Delta_t^2 \delta_z \delta_x e_z|^{n+\frac{1}{2}} \end{aligned} \quad (63)$$

and

$$\begin{aligned} [4 - c^2 \Delta_t^2 \delta_x^2] h_z|^{n+1} = 4h_z|^{n+\frac{1}{2}} + \\ 2c\Delta_t[\delta_y e_x|^{n+\frac{1}{2}} - \delta_x e_y|^{n+\frac{1}{2}}] - c^2 \Delta_t^2 \delta_x \delta_z h_x|^{n+\frac{1}{2}}. \end{aligned} \quad (64)$$

From the set of six equations for the first half step only the first three of type (61) for $e_x|^{n+\frac{1}{2}}$, $e_y|^{n+\frac{1}{2}}$, $e_z|^{n+\frac{1}{2}}$ have to be solved since having obtained these values the values for $h_x|^{n+\frac{1}{2}}$, $h_y|^{n+\frac{1}{2}}$, $h_z|^{n+\frac{1}{2}}$ can be easily obtained from the second three equations of type (58).

Analogously for the second half step only the solution of the last three equations of type (64) for $h_x|^{n+1}$, $h_y|^{n+1}$, $h_z|^{n+1}$ is required and $e_x|^{n+1}$, $e_y|^{n+1}$, $e_z|^{n+1}$ are determined from first three equations of type (59).

The calculation can be further re-organised in a “leapfrog” way [10]. When the direction of the time axis in (61) is reversed around the point n , *ie* $n + \frac{1}{2} \Rightarrow n - \frac{1}{2}$, $c\Delta_t \Rightarrow -c\Delta_t$, and subtracting the result from (61) one arrives at the “leapfrog” algorithm [10]

$$\begin{aligned} [4 - c^2 \Delta_t^2 \delta_y^2] e_x|^{n+\frac{1}{2}} = \\ [4 - c^2 \Delta_t^2 \delta_y^2] e_x|^{n-\frac{1}{2}} + 4c\Delta_t[\delta_y h_z|^n - \delta_z h_y|^n] \end{aligned} \quad (65)$$

Similarly the reversal of the time axis in (64) around the point $n + \frac{1}{2}$, *ie* $n + 1 \Rightarrow n$, $c\Delta_t \Rightarrow -c\Delta_t$, and subtracting the result from (64) gives

$$\begin{aligned} [4 - c^2 \Delta_t^2 \delta_x^2] h_z|^{n+1} = \\ [4 - c^2 \Delta_t^2 \delta_x^2] 4h_z|^n + 4c\Delta_t[\delta_y e_x|^{n+\frac{1}{2}} - \delta_x e_y|^{n+\frac{1}{2}}]. \end{aligned} \quad (66)$$

The equations for other components $e_y|^{n+\frac{1}{2}}$ and $e_z|^{n+\frac{1}{2}}$ are obtained by cyclic permutation in (65) and similarly from (66) the equations for $h_x|^{n+1}$ and $h_y|^{n+1}$.

As pointed out in [10] an additional benefit is the absence of the mixed difference terms in (65) and (66) on the contrary to (61) through (64), where the terms $\delta_y \delta_x e_y|^n$, $\delta_z \delta_y h_y|^n$, $\delta_z \delta_x e_z|^n$, $\delta_x \delta_z h_x|^n$ occur. Observe also that in the limit $c\Delta_t \rightarrow 0$ the implicit equations (65) and (66) approach the explicit equations (11) and (12).

In fact (65) actually means

$$\begin{aligned} b_y^2 e_x|_{i+\frac{1}{2},j+1,m}^{n+\frac{1}{2}} - 2(2 + b_y^2) e_x|_{i+\frac{1}{2},j,m}^{n+\frac{1}{2}} + b_y^2 e_x|_{i+\frac{1}{2},j-1,m}^{n+\frac{1}{2}} \\ = b_y^2 e_x|_{i+\frac{1}{2},j+1,m}^{n-\frac{1}{2}} - 2(2 + b_y^2) e_x|_{i+\frac{1}{2},j,m}^{n-\frac{1}{2}} + b_y^2 e_x|_{i+\frac{1}{2},j-1,m}^{n-\frac{1}{2}} \\ - 4b_y (h_z|_{i+\frac{1}{2},j+\frac{1}{2},m}^n - h_z|_{i+\frac{1}{2},j-\frac{1}{2},m}^n) \\ + 4b_z (h_y|_{i+\frac{1}{2},j,m,\frac{1}{2}}^n - h_y|_{i+\frac{1}{2},j,m,-\frac{1}{2}}^n), \end{aligned} \quad (67)$$

and (66) actually means

$$\begin{aligned} b_x^2 h_z|_{i+\frac{3}{2},j+\frac{1}{2},m}^{n+1} - 2(2 + b_x^2) h_z|_{i+\frac{1}{2},j+\frac{1}{2},m}^{n+1} + b_x^2 h_z|_{i-\frac{1}{2},j+\frac{1}{2},m}^{n+1} = \\ b_x^2 h_z|_{i+\frac{3}{2},j+\frac{1}{2},m}^n - 2(2 + b_x^2) h_z|_{i+\frac{1}{2},j+\frac{1}{2},m}^n + b_x^2 h_z|_{i-\frac{1}{2},j+\frac{1}{2},m}^n \\ - 4b_y (e_x|_{i+\frac{1}{2},j+1,m}^{n+\frac{1}{2}} - e_x|_{i+\frac{1}{2},j,m}^{n+\frac{1}{2}}) \\ + 4b_x (e_y|_{i+1,j+\frac{1}{2},m}^{n+\frac{1}{2}} - e_y|_{i,j+\frac{1}{2},m}^{n+\frac{1}{2}}) \end{aligned} \quad (68)$$

where the left sides represent the elements of the tridiagonal matrix to be solved. The tridiagonal equations for the other components $e_y|^{n+\frac{1}{2}}$, $e_z|^{n+\frac{1}{2}}$, $h_x|^{n+1}$ and $h_y|^{n+1}$ are easily obtained from (67) and (68) by cyclic permutation of indices.

The forward-marching algorithm provided by the solution of these two sets, each of three tri-diagonal equations, proceeds similarly as in the Yee’s explicit algorithm — compare (67) with (11) and (68) with (12) — in a “leapfrog” way, *ie* the values $e_{x,y,z}|^{n+\frac{1}{2}}$, $h_{x,y,z}|^{n+1}$,

$e_{x,y,z}|^{n+\frac{3}{2}}$, $h_{x,y,z}|^{n+2}$ etc are subsequently obtained from the values in two preceding time layers.

In two dimensions for the TE wave the pertaining “leapfrog” equations for the e_x and e_z in the first step read

$$e_x|_{i+\frac{1}{2},m}^{n+\frac{1}{2}} = e_x|_{i+\frac{1}{2},m}^{n-\frac{1}{2}} - b_z(h_y|_{i+\frac{1}{2},m+\frac{1}{2}}^n - h_y|_{i+\frac{1}{2},m-\frac{1}{2}}^n), \quad (69)$$

$$\begin{aligned} b_x^2 e_z|_{i+1,m+\frac{1}{2}}^{n+\frac{1}{2}} - 2(2 + b_x^2) e_z|_{i,m+\frac{1}{2}}^{n+\frac{1}{2}} + b_x^2 e_z|_{i-1,m+\frac{1}{2}}^{n+\frac{1}{2}} = \\ b_x^2 e_z|_{i+1,m+\frac{1}{2}}^{n-\frac{1}{2}} - 2(2 + b_x^2) e_z|_{i,m+\frac{1}{2}}^{n-\frac{1}{2}} + b_x^2 e_z|_{i-1,m+\frac{1}{2}}^{n-\frac{1}{2}} \\ - 4b_x(h_y|_{i+\frac{1}{2},m+\frac{1}{2}}^n - h_y|_{i-\frac{1}{2},m+\frac{1}{2}}^n), \end{aligned} \quad (70)$$

while for h_y in the second step one obtains

$$\begin{aligned} b_z^2 h_y|_{i+\frac{1}{2},m+\frac{3}{2}}^{n+1} - 2(2 + b_z^2) h_y|_{i+\frac{1}{2},m+\frac{1}{2}}^{n+1} + b_z^2 h_y|_{i+\frac{1}{2},m-\frac{1}{2}}^{n+1} = \\ b_z^2 h_y|_{i+\frac{1}{2},m+\frac{3}{2}}^n - 2(2 + b_z^2) h_y|_{i+\frac{1}{2},m+\frac{1}{2}}^n + b_z^2 h_y|_{i+\frac{1}{2},m-\frac{1}{2}}^n \\ - 4b_x(e_z|_{i+1,m+\frac{1}{2}}^{n+\frac{1}{2}} - e_z|_{i,m+\frac{1}{2}}^{n+\frac{1}{2}}) + 4b_z(e_x|_{i+\frac{1}{2},m+1}^{n+\frac{1}{2}} - e_x|_{i+\frac{1}{2},m}^{n+\frac{1}{2}}). \end{aligned} \quad (71)$$

For the TM wave holds analogously

$$\begin{aligned} b_z^2 e_y|_{i,m+1}^{n+\frac{1}{2}} - 2(2 + b_z^2) e_y|_{i,m}^{n+\frac{1}{2}} + b_z^2 e_y|_{i,m-1}^{n+\frac{1}{2}} = \\ b_z^2 e_y|_{i,m+1}^{n-\frac{1}{2}} - 2(2 + b_z^2) e_y|_{i,m}^{n-\frac{1}{2}} + b_z^2 e_y|_{i,m-1}^{n-\frac{1}{2}} + \\ 4b_x(h_z|_{i+\frac{1}{2},m+1}^n - h_z|_{i+\frac{1}{2},m-1}^n) - 4b_z(h_x|_{i,m+\frac{1}{2}}^n - h_x|_{i,m-\frac{1}{2}}^n). \end{aligned} \quad (72)$$

$$h_x|_{i,m+\frac{1}{2}}^{n+1} = h_x|_{i,m+\frac{1}{2}}^n + b_z(e_y|_{i,m+1}^{n+\frac{1}{2}} - e_y|_{i,m}^{n+\frac{1}{2}}), \quad (73)$$

$$\begin{aligned} b_x^2 h_z|_{i+\frac{3}{2},m}^{n+1} - 2(2 + b_x^2) h_z|_{i+\frac{1}{2},m}^{n+1} + b_x^2 h_z|_{i-\frac{1}{2},m}^{n+1} = \\ b_x^2 h_z|_{i+\frac{3}{2},m}^n - 2(2 + b_x^2) h_z|_{i+\frac{1}{2},m}^n + b_x^2 h_z|_{i-\frac{1}{2},m}^n \\ - 4b_x(e_y|_{i+1,m}^{n+\frac{1}{2}} - e_y|_{i,m}^{n+\frac{1}{2}}). \end{aligned} \quad (74)$$

Observe that for TE as well as for TM wave only one equation have to be solved for each Δ_t step since (69) and (73) give $e_x|_{i+\frac{1}{2},m}^{n+\frac{1}{2}}$ and $h_x|_{i,m+\frac{1}{2}}^{n+1}$ in an explicit way.

7 THE APPROXIMATE IMPLICIT FORMULATION: THE CNSS-FDTD METHOD

Alternatively can (44) be expressed in the following way

$$\begin{aligned} \left\{ \mathbf{I} - \frac{c\Delta_t}{2} (\mathbf{D}_{12} - \mathbf{D}_{21}) \right\} \mathbf{f}^{n+1} = \\ = \left\{ \mathbf{I} + \frac{c\Delta_t}{2} (\mathbf{D}_{12} - \mathbf{D}_{21}) \right\} \mathbf{f}^n \end{aligned} \quad (75)$$

and then similarly as in (53) be re-cast into the form

$$\begin{aligned} \left\{ \mathbf{I} - \frac{c\Delta_t}{2} \mathbf{D}_{12} \right\} \left\{ \mathbf{I} + \frac{c\Delta_t}{2} \mathbf{D}_{21} \right\} \mathbf{f}^{n+1} + \\ + \frac{c^2 \Delta_t^2}{4} \mathbf{D}_{12} \mathbf{D}_{21} \mathbf{f}^{n+1} = \\ = \left\{ \mathbf{I} + \frac{c\Delta_t}{2} \mathbf{D}_{12} \right\} \left\{ \mathbf{I} - \frac{c\Delta_t}{2} \mathbf{D}_{21} \right\} \mathbf{f}^n \\ + \frac{c^2 \Delta_t^2}{4} \mathbf{D}_{12} \mathbf{D}_{21} \mathbf{f}^n. \end{aligned} \quad (76)$$

After having neglected last terms on RHS and LHS of (76) one again arrives to analogous equation as (54)

$$\begin{aligned} \left\{ \mathbf{I} - \frac{c\Delta_t}{2} \mathbf{D}_{12} \right\} \left\{ \mathbf{I} + \frac{c\Delta_t}{2} \mathbf{D}_{21} \right\} \mathbf{f}^{n+1} = \\ \left\{ \mathbf{I} + \frac{c\Delta_t}{2} \mathbf{D}_{12} \right\} \left\{ \mathbf{I} - \frac{c\Delta_t}{2} \mathbf{D}_{21} \right\} \mathbf{f}^n, \end{aligned} \quad (77)$$

which can again be splitted into two subsequent steps

$$\left\{ \mathbf{I} + \frac{c\Delta_t}{2} \mathbf{D}_{21} \right\} \mathbf{f}^* = \left\{ \mathbf{I} - \frac{c\Delta_t}{2} \mathbf{D}_{21} \right\} \mathbf{f}^n, \quad (78)$$

$$\left\{ \mathbf{I} - \frac{c\Delta_t}{2} \mathbf{D}_{12} \right\} \mathbf{f}^{n+1} = \left\{ \mathbf{I} + \frac{c\Delta_t}{2} \mathbf{D}_{12} \right\} \mathbf{f}^*. \quad (79)$$

This procedure is called Crank-Nicolson-Split-Step (CNSS) FDTD method. In both methods, ADI-FDTD and CNSS-FDTD, the terms of the second order on the RHS and the LHS of (53) and (76) are neglected. Therefore both are in Δ_t second order approximate in comparison with the full Crank-Nicolson formulation (52) or (75).

The first and the last equation of (78) after the spatial discretisation read

$$2(e_x|^{n+\frac{1}{2}} - e_x|^{n}) = c\Delta_t(\delta_y h_z|^{n+\frac{1}{2}} + \delta_y h_z|^{n}), \quad (80)$$

$$2(h_z|^{n+\frac{1}{2}} - h_z|^{n}) = c\Delta_t(\delta_y e_x|^{n+\frac{1}{2}} + \delta_y e_x|^{n}). \quad (81)$$

The first and the last equation of (79) are

$$2(e_x|^{n+1} - e_x|^{n+\frac{1}{2}}) = -c\Delta_t(\delta_z h_y|^{n+\frac{1}{2}} + \delta_z h_y|^{n+1}), \quad (82)$$

$$2(h_z|^{n+1} - h_z|^{n+\frac{1}{2}}) = -c\Delta_t(\delta_x e_y|^{n+\frac{1}{2}} + \delta_x e_y|^{n+1}). \quad (83)$$

In a similar way as in preceding paragraph the algorithm can be organised in a tridiagonal matrix for the first half-step analogous to (61) and (62)

$$[4 - c^2 \Delta_t^2 \delta_y^2] e_x |^{n+\frac{1}{2}} = [4 + c^2 \Delta_t^2 \delta_y^2] e_x |^n + 4c \Delta_t \delta_y h_z |^n, \quad (84)$$

$$[4 - c^2 \Delta_t^2 \delta_y^2] h_z |^{n+\frac{1}{2}} = [4 + c^2 \Delta_t^2 \delta_y^2] h_z |^n + 4c \Delta_t \delta_y e_x |^n, \quad (85)$$

and for the second half-step analogous to (63) and (64)

$$[4 - c^2 \Delta_t^2 \delta_z^2] e_x |^{n+1} = [4 + c^2 \Delta_t^2 \delta_z^2] e_x |^{n+\frac{1}{2}} - 4c \Delta_t \delta_z h_y |^{n+\frac{1}{2}}, \quad (86)$$

$$[4 - c^2 \Delta_t^2 \delta_x^2] h_z |^{n+1} = [4 + c^2 \Delta_t^2 \delta_x^2] h_z |^{n+\frac{1}{2}} - 4c \Delta_t \delta_x e_y |^{n+\frac{1}{2}}. \quad (87)$$

The “leapfrog” algorithm can be obtained in an analogous way as (66) and (65) with the result

$$[4 - c^2 \Delta_t^2 \delta_y^2] e_x |^{n+\frac{1}{2}} = [4 - c^2 \Delta_t^2 \delta_y^2] e_x |^{n-\frac{1}{2}} + 8c \Delta_t \delta_y h_z |^n, \quad (88)$$

$$[4 - c^2 \Delta_t^2 \delta_x^2] h_z |^{n+1} = [4 - c^2 \Delta_t^2 \delta_x^2] 4h_z |^n - 8\Delta_t \delta_x e_y |^{n+\frac{1}{2}}. \quad (89)$$

Written down explicitly, (88) and (89) takes the form

$$\begin{aligned} & b_y^2 e_x |_{i+\frac{1}{2}, j+1, m}^{n+\frac{1}{2}} - 2(2 + b_y^2) e_x |_{i+\frac{1}{2}, j, m}^{n+\frac{1}{2}} + b_y^2 e_x |_{i+\frac{1}{2}, j-1, m}^{n+\frac{1}{2}} = \\ & = b_y^2 e_x |_{i+\frac{1}{2}, j+1, m}^{n-\frac{1}{2}} - 2(2 + b_y^2) e_x |_{i+\frac{1}{2}, j, m}^{n-\frac{1}{2}} + b_y^2 e_x |_{i+\frac{1}{2}, j-1, m}^{n-\frac{1}{2}} \\ & \quad - 8b_y (h_z |_{i+\frac{1}{2}, j, m+\frac{1}{2}}^n - h_z |_{i+\frac{1}{2}, j, m-\frac{1}{2}}^n), \end{aligned} \quad (90)$$

$$\begin{aligned} & b_x^2 h_z |_{i+\frac{3}{2}, j+\frac{1}{2}, m}^{n+1} - 2(2 + b_x^2) h_z |_{i+\frac{1}{2}, j+\frac{1}{2}, m}^{n+1} + b_x^2 h_z |_{i-\frac{1}{2}, j+\frac{1}{2}, m}^{n+1} = \\ & = b_x^2 h_z |_{i+\frac{3}{2}, j+\frac{1}{2}, m}^n - 2(2 + b_x^2) h_z |_{i+\frac{1}{2}, j+\frac{1}{2}, m}^n + b_x^2 h_z |_{i-\frac{1}{2}, j+\frac{1}{2}, m}^n \\ & \quad + 8b_x (e_y |_{i+\frac{1}{2}, j+1, m}^{n+\frac{1}{2}} - e_y |_{i+\frac{1}{2}, j, m}^{n+\frac{1}{2}}). \end{aligned} \quad (91)$$

The difference in leapfrog algorithm between ADI-FDTD (67),(68) and CNSS-FDTD (90),(91) is clearly visible, while in ADI-FDTD always both terms $\delta_y h_z |^n$, $\delta_z h_y |^n$, and $\delta_y e_x |^{n+\frac{1}{2}}$ respectively, are present in CNSS-FDTD only $\delta_y h_z |^n$ in (90) or $\delta_x e_y |^{n+\frac{1}{2}}$ in (91) occur.

7 POWER CONSERVATION AND THE NUMERICAL DISPERSION OF THE IMPLICIT SCHEMES

For the sake of simplicity let us consider the two-dimensional case only. Using the von Neumann’s procedure for investigating the power-conservation and numerical-dispersion properties of respective algorithms one obtains for the full Crank Nicolson formulation of the FDTD method the equation

$$(1 + A_x^2 + A_z^2) \xi^2 - 2(1 - A_x^2 - A_z^2) \xi + 1 = 0 \quad (92)$$

with the solution

$$\xi = \frac{1 - A_x^2 - A_z^2 - j2\sqrt{A_x^2 + A_z^2}}{1 + A_x^2 + A_z^2}, \quad (93)$$

For the ADI-FDTD for each of two simulation-half-steps $\Delta_t/2$ the following equation is obtained

$$(1 + A_{x,z}^2) \xi_{1,2} - 2\sqrt{\xi_{1,2}} + (1 + A_{z,x}^2) = 0 \quad (94)$$

with the solution

$$\sqrt{\xi_{1,2}} = \frac{1 - j\sqrt{(1 + A_{x,z}^2)(1 + A_{z,x}^2)} - 1}{1 + A_{x,z}^2}, \quad (95)$$

ie for the full step $\xi = \sqrt{\xi_1 \xi_2}$.

For the CNSS-FDTD method one similarly obtains for respective half-steps the equation

$$(2 + A_{x,z}^2) \xi_{1,2} - 2(2 - A_{x,z}^2) \sqrt{\xi_{1,2}} + (2 + A_{z,x}^2) = 0 \quad (96)$$

with the solution

$$\sqrt{\xi_{1,2}} = \frac{\{2 - A_{x,z}^2\} - j2\sqrt{2}A_{x,z}}{2 + A_{x,z}^2}. \quad (97)$$

The power-flow-density for the full step Δ_t is in all cases unconditionally conserved since either in (93) $|\xi| = 1$, or in (95) and (97) $|\xi| = |\sqrt{\xi_1}| |\sqrt{\xi_2}| = 1$, holds.

The dispersion characteristics are fully determined by the phase of ξ , $\omega \Delta_t = -\text{phase}(\xi)$, ie in the case of full Crank-Nicolson formulation (93) by

$$\omega \Delta_t = \arccos \frac{1 - A_x^2 - A_z^2}{1 + A_x^2 + A_z^2}, \quad (98)$$

in the case of ADI-FDTD by

$$\omega \Delta_t = 2 \arccos \frac{1}{\sqrt{(1 + A_x^2)(1 + A_z^2)}} \quad (99)$$

and in the case CNSS-FDTD by

$$\omega \Delta_t = \arccos \frac{2 - A_x^2}{2 + A_x^2} + \arccos \frac{2 - A_z^2}{2 + A_z^2} \quad (100)$$

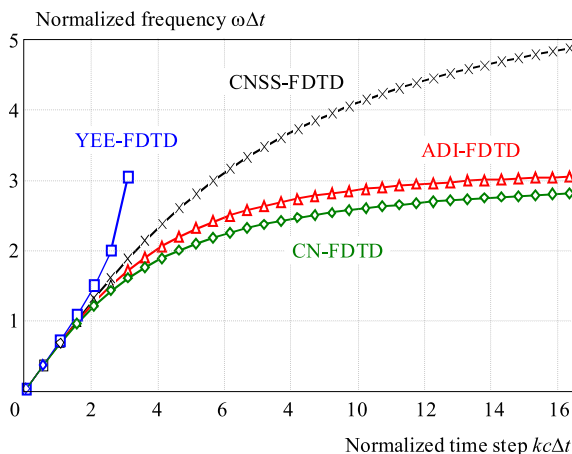


Fig. 4. Dependence of the normalised frequency $\omega\Delta t$ on the normalised time step $kc\Delta t$, for $k_x\Delta_x = k_z\Delta_z = 3$ and the propagation angle $\arctan(k_z/k_x) = 0.262$

For the explicit Yee-FDTD the values can be calculated until the Courant limit is reached. Here the simulated frequency arrives at the limit given by the sampling theorem $\omega\Delta t = \pi$. For CN-FDTD and ADI-FDTD the sampling theorem limit $\omega\Delta t \rightarrow \pi$ is approached asymptotically with increasing Δt . For CNSS-FDTD the limit for large Δt is equal to $\omega\Delta t \rightarrow 2\pi$. One has to keep in mind that for $\omega\Delta t > \pi$ the aliasing effects occur.

Generally the phase velocity and the group velocity for implicit methods decrease with increasing time-step Δt . The possibility of the arbitrarily large Δt steps in the ADI-FDTD and CNSS-FDTD method does not necessarily mean any advantage, since with growing Δt the phase velocity $v_p = \text{phase}(\xi)/k\Delta t$ decreases, *ie* the simulated spatial propagation path pertaining to increased time step remains effectively the same.

As seen from the comparison of curves for CN-FDTD and ADI-FDTD they are very close. *ie* the ADI-FDTD method well approximates the results for the full CN-FDTD method. Neglecting the second order terms in the factorization (55), (56) does not cause any substantial error in dispersion characteristics unlike the CNSS-FDTD where the factorization (78), (79) leads to larger numerical dispersion errors.

8 CONCLUSIONS

In this second part of the short tutorial the selected aspects of computer simulation of electromagnetic wave

phenomena in two and three dimensions have been thoroughly discussed. We have focused mainly on the power conservation and the numerical dispersion properties of particular methods.

REFERENCES

- [1] ŠUMICHRAST, .: On Some Strategies for Computer Simulation of the Wave Propagation using Finite Differences, I. One-Dimensional FDTD Method, J. Electrical Engineering **64** No. 4 (2013), 212–221.
- [2] YEE, K. S. : Numerical Solution of Initial Boundary Value Problems Involving Maxwell's Equations in Isotropic Media, IEEE Trans. on Antennas and Prop. **AP-14** No. 3, (1966), 302–307.
- [3] BI, Z.—WU, K.—WU, C.—LITVA, J. : A New Finite-Difference Time-Domain Algorithm for Solving Maxwell's Equations, IEEE Microwave & Guided Wave Lett. **1** No. 12 (1991), 382–384.
- [4] NAMIKI, T. : A New FDTD Algorithm based on Alternating-Direction Implicit Method, IEEE Trans. Microwave Theory & Techn. **MTT-47** No. 10 (1999), 2003–2007.
- [5] ZHENG, F.—CHEN, Z.—ZHANG, J. : A Finite-Difference Time-Domain Method without the Courant Stability Conditions, IEEE Microwave & Guided Wave Lett. **9** (1999), 441–443.
- [6] ZHENG, F.—CHEN, Z.—ZHANG, J. : Toward the Development of a Three-Dimensional Unconditionally Stable Finite-Difference Time-Domain Method, IEEE Trans. Microwave Theory & Techn. **MTT-48** No. 9 (2000), 1550–1558.
- [7] LEE, J.—FORNBERG, B. : A Split Step Approach for the 3 D Maxwell's Equations, J. Comp. Appl. Math. **158** (2003), 185–505.
- [8] LEE, J.—FORNBERG, B. : Some Unconditionally Stable Time Stepping Methods for the 3D Maxwell's Equations, J. Comp. & Appl. Math. **166** (2004), 497–52.
- [9] GARCIA, S. G.—RUBIO, R. G.—BRETONES, A. R.—MARTIN, R. G. : On the Dispersion Relation of ADI-FDTD, IEEE Microwave & Wireless Prop. Lett. **16** (2006), 354–356.
- [10] COOKE, S. J.—BOTTON, M.—ANTONSEN, T. M. Jr.—LEVUSH, B. : A Leapfrog Formulation of the 3D ADI-FDTD Algorithm, , Int. J. Numer. Model. **22** (2009), 187–200.

Received 6 January 2013

Ľubomír Šumichrast is with the Faculty of Electrical Engineering and Information Technology of the Slovak University of Technology since 1971, now holding the position of an Associate Professor and Deputy director of the Institute of Electrical Engineering. He spent the period 1990-1992 as a visiting professor at the University Kaiserslautern, Germany and spring semester 1999 as a visiting professor at the Technical University Ilmenau, Germany. His main research interests include the electromagnetic waves propagation in various media and structures, computer modelling of wave propagation effects as well as optical communication and integrated optics.